Optimized Walking Control of a Biped Walking Robot Considering Theory of a Pendulum

Hisashi Koike, Jae Hoon Lee[1], and Shingo Okamoto

Ehime University, Japan
(Tel: 81-089-927-9740, Fax: 81-089-927-9740)

[1]jhlee@ehime-u.ac.jp

Abstract: A motion control based on the theory of passive walking has been investigated in this paper. It has been known that general passive walking robot can walk efficiently on the slope by using potential energy with no actuator. However, it cannot walk on the horizontal ground. In order to utilize the merit of energy efficiency, two motors were installed at the hip joints of the passive-walking-type robot, which generate required torque for walking on the horizontal ground. The proportional control algorithm was applied for successive walking. Computer simulations with its dynamic model were carried out to find out the optimal condition for walking motion. Based on the simulation results, experimental robot was developed. As a result, the capability of walking on the horizontal ground was confirmed through experimental works with the proposed method and the developed robot.

Keywords: Biped walking robot, Passive walking, Walking control.

1 INTRODUCTION

Recent biped robot shows advanced performance in their motion, especially in walking. However, it has been known that the energy efficiency of typical biped robots in walking motion is worse than human [1]. Therefore, walking efficiency has been considered as an important issue for innovation of humanoid robot. Passive walking robot has been investigated as a model to understand and solve the problem [2]. The passive walking robot can walk efficiently on the slope by using their passive legs which rotate like as pendulums. However, it can't walk on the horizontal ground because it has no energy source to move its leg forward.

This research aims to develop the biped walking robot that can walk on the horizontal ground. Besides, to improve walking efficiency, the theory of passive walking is also considered. For that, the minimum number of actuators, i.e. two motors, were installed at the hip joints of the robot, which generate the control torques for walking motion. In the previous researches [3,4], the computer simulations with dynamic model were carried out to investigate the walking capability of the system. In this research, the experimental system with embedded controller has been developed. The system with the proposed method was investigated through experimental works.

2 COMPUTER SIMULATION

The computer simulations with the dynamic model of the biped robot with a torso were performed [4].

2.1 Analysis model

Figure 1 shows the analysis model of the walking robot. The robot consists of a torso, a hip and two legs with feet. By alternating the state of both legs between stance and swing, the robot can walk successively. For generating torque for walking motion, two motors are installed at the hip joints. Where τ_1 and τ_2 denote the control torque between the stance-leg and the torso, and the torque the swing-leg and the torso, respectively.

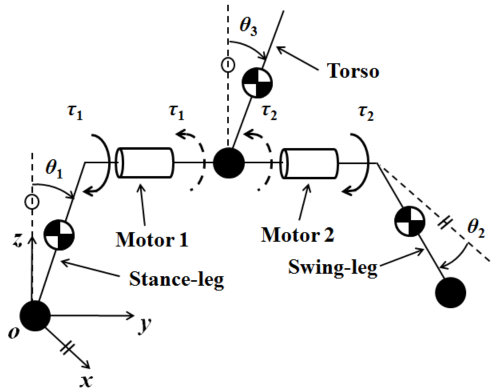

Fig. 1. Analysis model of the walking robot with motors [4]

2.2 Equation of motion

The motion equation of the robot is given by

$$\boldsymbol{M}(\boldsymbol{\theta})\ddot{\boldsymbol{\theta}} + \left[\boldsymbol{C}_c\left(\boldsymbol{\theta},\dot{\boldsymbol{\theta}}\right) + \boldsymbol{C}_d\right]\dot{\boldsymbol{\theta}} + \boldsymbol{g}(\boldsymbol{\theta}) = \boldsymbol{B}\boldsymbol{\tau} \qquad (1)$$

where, $\boldsymbol{\theta} = \{\theta_1 \quad \theta_2 \quad \theta_3\}^T$, $\boldsymbol{\tau} = \{\tau_1 \quad \tau_2\}$, $\boldsymbol{M}$ is the inertia matrix, $\boldsymbol{C}_c$ is a Coriolis and centrifugal force matrix, $\boldsymbol{C}_d$ is a viscosity damping matrix, $\boldsymbol{B}$ is a coefficient matrix about control torque, and $\boldsymbol{g}$ is the gravity vector, respectively.

2.3 Exchange between stance leg and swing leg

The condition of the touchdown of the swing-leg is given by

$$\theta_1 + \theta_2 = \pi / 2 . \qquad (2)$$

The contact between the swing-leg and the ground when the swing-leg passes through the stance-leg was ignored.

Then the impact at the touchdown was assumed to be inelastic. It was also assumed that the stance-leg leaves from the ground at the moment of touchdown.

The angular velocity of the joints after touchdown is computed as follows. The angular momentum is conserved before and after touchdown for the whole robot about the leading contact point, the trailing leg about the hip and the torso about the hip. Equation (3) is given by these conservation laws of angular momentum:

$$\boldsymbol{Q}^{+}(\boldsymbol{\theta}^{+})\dot{\boldsymbol{\theta}}^{+} = \boldsymbol{Q}^{-}(\boldsymbol{\theta}^{-})\dot{\boldsymbol{\theta}}^{-} . \tag{3}$$

The superscripts "-" and "+" denote the state before and after touchdown, respectively. The relation of the angles before and after touchdown is given by

$$\boldsymbol{\theta}^{+} = \boldsymbol{R}\boldsymbol{\theta}^{-} + \boldsymbol{\theta_0} , \tag{4}$$

where

$$\boldsymbol{R} = \begin{bmatrix} 0 & 1 & 0 \\ 1 & 0 & 0 \\ 0 & 0 & 1 \end{bmatrix}, \tag{5}$$

$$\boldsymbol{\theta_0} = \{-\pi/2 \quad \pi/2 \quad 0\}^T , \tag{6}$$

Resultantly, the angular velocity of all joints after touchdown is calculated by

$$\dot{\boldsymbol{\theta}}^{+} = \boldsymbol{Q}^{+}(\boldsymbol{\theta}^{+})^{-1}\boldsymbol{Q}^{-}(\boldsymbol{\theta}^{-})\dot{\boldsymbol{\theta}}^{-} . \tag{7}$$

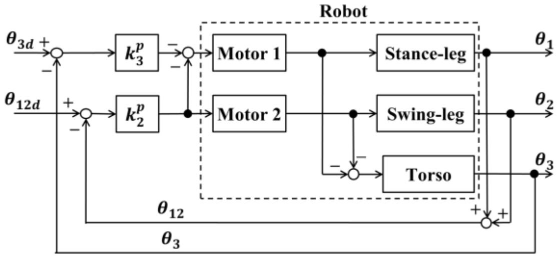

Fig. 2. Block diagram of active control for calculations [4]

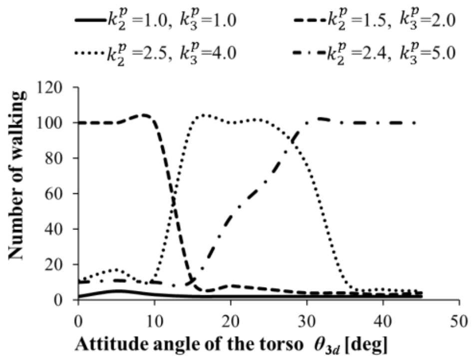

Fig. 3. Relation between control gains and the number of walking [4]

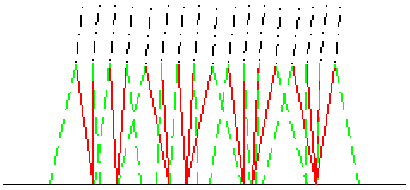

Fig. 4. Walking motion using PD control [4]

2.4 Motion control

The proportional (P) and proportional-differential (PD) control law have been employed. In the case of proportional control, the control torques τ_1 and τ_2 are given by Eq. (8) and (9).

$$-\tau_1 - \tau_2 = k_3^p(\theta_{3d} - \theta_3), \tag{8}$$

$$\tau_2 = k_2^p(\theta_{12d} - \theta_{12}), \tag{9}$$

where

$$\theta_{12} = \theta_1 + \theta_2 , \tag{10}$$

$$\theta_{12d} = \pi/2 . \tag{11}$$

The k_2^p and k_3^p denotes the control gains. The control torque τ_1 is given by

$$\tau_1 = -k_2^p(\theta_{12d} - \theta_{12}) - k_3^p(\theta_{3d} - \theta_3). \tag{12}$$

The block diagram of active control for calculation is shown in Fig. 2, where the proportional control is used.

2.5 Result of computer simulation

The optimal control gains have been found out through simulations with various conditions. Figure 3 shows the relation between θ_{3d} and the number of successive walking motion. An example of the calculated results is given in Fig. 4.

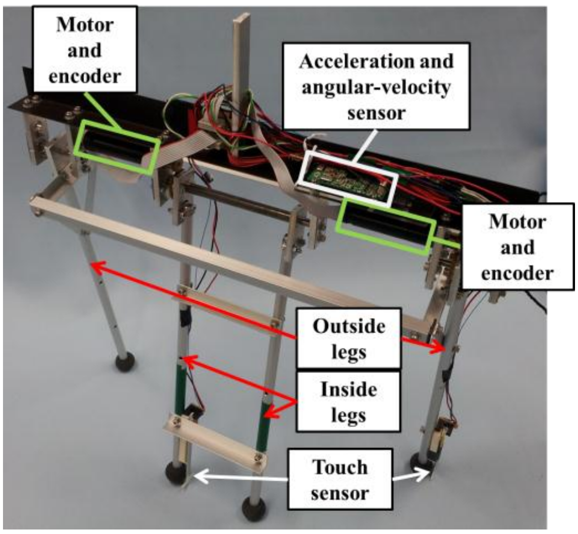

Fig. 5. Experimental robot

3 DEVELOPMENT OF EXPERIMENTAL ROBOT

3.1 Composition of the robot

Figure 5 shows the experimental robot which was developed based on the result of computer simulation. The length of each leg and the torso are 310 [mm] and 140 [mm], respectively. The total mass of whole system is 0.65 [kg]. In order to constrain the walking motion in the vertical planar space, each leg consists of two parallel links. So the inside legs and the outside legs are connected with each other by additional frames, respectively. The control torques are generated by the motors installed at the hip joints. The encoders are installed at the motors to measure the angle of each hip joint. The attitude angle of the torso is measured by the attitude sensor (HiBot Co., Japan) attached on the torso. Two micro controllers were employed for motion control and computation of sensor information. Their photographs are given in Fig. 6. Two touch sensors were attached on both, i.e. inside and outside, the feet to detect the contact between the feet and the ground. Figure 7 shows the touch sensor attached on the foot.

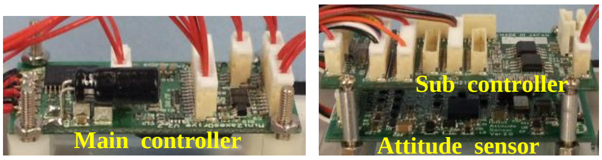

Fig. 6. Controller and attitude sensor

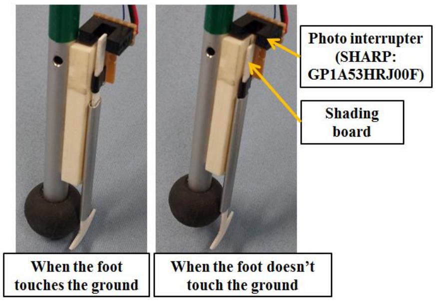

Fig. 7. Touch sensor on the foot

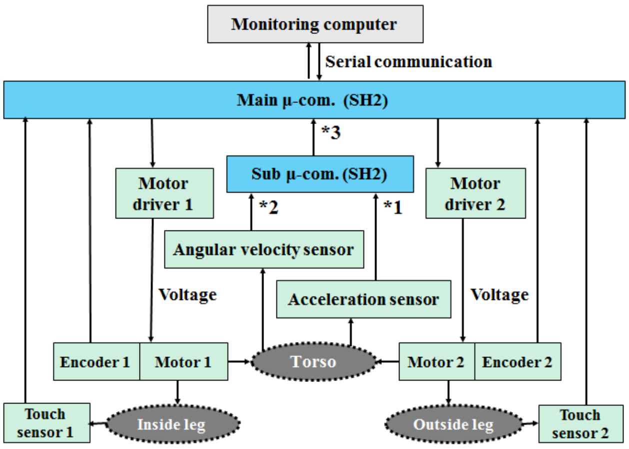

*1 : Accelerations (x'-, y'- and z'-directions)
*2 : Angular velocities (about x'- and y'-axes)
*3 : Attitude angle θ_3 of torso

Fig. 8. System configuration of the experimental robot

3.2 System configuration

Figure 6 shows the system configuration of the experimental robot. The robot has two embedded controllers. The main controller is for motor control, and the other, sub controller, is for the attitude sensor. They are connected by CAN communication channel with each other. Besides, the information about motion and sensors is transferred from the main controller to a monitoring computer outside the robot through serial communication channel.

State of the robot is recognized by values of two touch sensors. The angle of the torso, θ_3, is achieved by the sub controller and the attitude sensor that measures the acceleration and angular velocity [5]. This angle is sent to main controller and used for motion control. From the encoders of motors, relative angles between the torso and each leg are measured. The absolute angle of each leg, θ_1 and θ_2, are computed with the attitude angle of the torso and two encoder values, which is used in the feedback control for walking. While the robot moves, all sensor information is sent to monitoring computer in real time. The sampling time of the motor control is set to 1 [ms]. The frequency of communication between main controller and the monitoring computer is set to 100 [Hz].

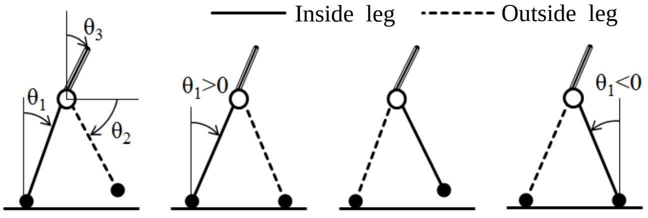

(a)Inside leg is stance leg
(b)Both legs are stance leg ($\theta_1>0$)
(c)Outside leg is stance leg
(d)Both legs are stance leg ($\theta_1<0$)

Fig. 9. The states of the experimental robot

4 WALKING EXPERIMENT

The developed robot system with the proposed method has been confirmed through experiments of walking on the horizontal ground.

4.1 Motion control for walking experiment

In simulation, the stance-leg was assumed to leave from the ground at the moment of the touchdown. However, in the actual walking motion, there exists the period that both legs are in stance state. Therefore, motion control method for the real robot needs to be modified as follows. Walking motion of the real robot is divided into four states according to the values of the touch sensors and the angle of the legs as shown in Fig. 9. The states are as follows.

(a) The inside leg is stance leg.
(b) The outside leg is stance leg.
(c) The both legs are stance legs and θ_1 is positive.
(d) The both legs are stance legs and θ_1 is negative.

Therefore, different control methods are applied according to the states as follows.

In the state (a) or (b), the control torques τ_1 and τ_2 are given as follows

$$\tau_1 = -k_3^p\left(\theta_{3d} - \theta_3\right), \tag{13}$$

$$\tau_2 = k_2^p\left(\theta_{2d} - \theta_2\right). \tag{14}$$

Where k_2^p and k_3^p denote the control gains. The θ_{2d} and θ_{3d} denote the desired angles.

In the state (c) or (d), the control torques τ_1 and τ_2 are given as follows

$$\tau_1 = k_2^p\left(\theta_{1d} - \theta_1\right), \tag{15}$$

$$\tau_2 = -k_3^p\left(\theta_{3d} - \theta_3\right). \tag{16}$$

The θ_{1d} denotes the desired angle.

The control torques are generated at the motors by the PWM (Pulse Width Modulation) signals from the main controller.

4.2 Experimental conditions

The initial posture and velocity is required for the robot when it starts its motion. In order to endow the robot with the same condition through the experiments, a special frame with pushing device was prepared. Besides, the contact between the swing-leg and the ground is occurred when the swing-leg passes through the angle of stance-leg because the length of both legs is same. To solve the problem, the blocks for feet are set on the ground as shown in Fig. 10.

4.3 Experimental result

The appropriate control gains had been found through experiments with the manner of trial and error. Resultantly, it has been observed that the robot can walk on the horizontal ground with the proposed method. The successive scene of the walking motion is shown in Fig. 10. It was captured with a high speed camera (CASIO: EX-FH25). The change of the angles θ_1, θ_2, θ_3 and the values of touch sensors are given in Fig. 11.

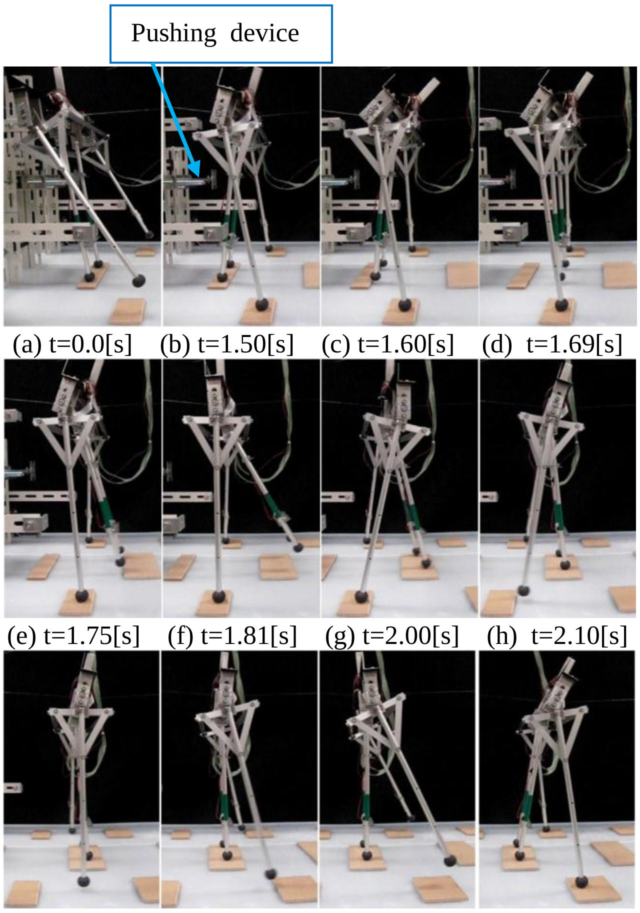

(a) t=0.0[s] (b) t=1.50[s] (c) t=1.60[s] (d) t=1.69[s]

(e) t=1.75[s] (f) t=1.81[s] (g) t=2.00[s] (h) t=2.10[s]

(i) t=2.19[s] (j) t=2.25[s] (k) t=2.31[s] (l) t=2.56[s]

($\theta_{1d} = -12$[deg], $\theta_{2d} = 78$[deg], $\theta_{3d} = 5$[deg], $k_2^p = 0.20\, k_3^p = 0.30$)

Fig. 10. Walking motion of experiment

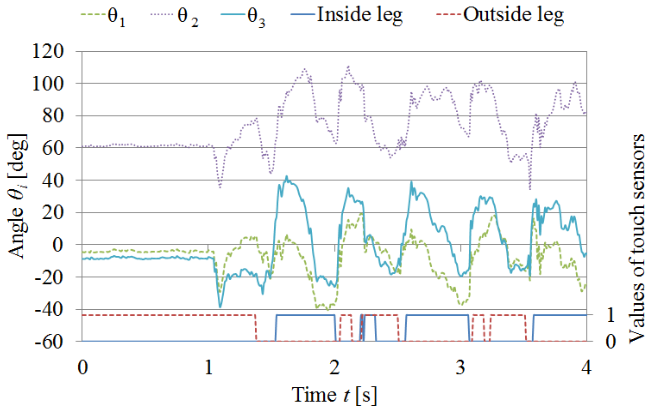

Fig. 11. The change of the joint angles and the values of touch sensors

5 CONCLUSION

The motion control based on passive walking theory had been investigated for biped walking on the horizontal ground. Considering the simulation results, the real robot system was developed. From experiments, it was found that there exists considerable difference between the ideal touchdown and that of real robot. Moreover, it adversely affects proper interchange between legs during touchdown. To cope with the problem, the walking motion was divided into four states. And the appropriate control algorithm for each state was applied in this paper. Resultantly, it was confirmed that the robot can walk on the horizontal ground with the proposed method.

The proposal of control algorithm for more stable walking and that for biped robot with knee joint will be carried out as future works.

REFERENCES

[1] Ono K and Liu R (2002), Optimal Biped Walking Locomotion Solved by Trajectory Planning Method. Journal of Dynamic Systems 124:554–565

[2] McGeer T (1990), Passive Dynamic Walking. The International Journal of Robotics Research 9:2:62-82

[3] Narukawa T, Takahashi M and Yoshida K (2010), Efficient waling with optimization for a planar biped walker with a torso by hip actuators and springs. Robotica 29:641–648

[4] Tani K, Okamoto S, Lee JH and Koike H (2012), Simulations on Motion Control and Development of Biped Walking Robot. Proceeding of the International MultiConference of Engineers and Computer Scientists 2012 2:916-919

[5] Ickowzcy E (2011), Design and Control of a Three-Wheeled Personal Vehicle with Active Suspension for Rough-Terrain Applications.